Conference Paper, Published Version

Haji Mohammadi, Mohammad; Mehran, Ali akbar; Pishva, Hooman

A New Modified Boundary Element Method (MBEM) for Boundary Domain Integral Method (BDIM)

MODIFIED BOUNDARY ELEMENT METHOD (MBEM) FOR BOUNDARY DOMAIN INTEGRAL METHOD (BDIM)

Mohammad Haji Mohammadi [1], Ali akbar Mehran [2], Hooman Pishva [3]

[1] Researcher, Department of Civil Engineering, Sharif University of Technology
P.O. Box 11365-9313, Tehran, Iran, e-mail:mhajit@gmail.com
[2] Research Student, Department of Mechanical and Environmental Informatics, Tokyo Institute of Technology
Ookayama, 2-12-1 Ookayama, Meguro-ku, Tokyo, JAPAN, 152-8552, e-mail: mehran@wv.mei.titech.ac.jp
[3] Research Student, Department of Civil Engineering, Azad University of Estahban
P.O. Box 74518-64747, Imam Reza Blvd, Estahban, Iran, e-mail: hooman.cfd@gmail.com

ABSTRACT

In this paper, a new and alternative method for Boundary Domain Integral Method (BDIM) in boundary elements method is represented for computation of incompressible viscous fluid flows, governed by the Navier-Stokes equation. Combined with dual reciprocity method (DRM), the proposed BEM algorithm uses vorticity–stream function formulation. To remove the probability of singular coefficient matrix, Hardy's Multiquadric radial basis function (RBF) with the shape parameter c=1 is employed in DRM algorithm. Spatial discretization is implemented by discretizing the boundary into linear elements. Adams method is employed for temporal discretization. Vorticity boundary conditions are constructed by Taylor's series second order expansion. Unlike usual BEMs for solving N-S equations, in which computation is done on whole domain (BDIM), except finite number of nodes in the Vicinity of boundary, no computation is needed in domain. The accuracy and robustness of the proposed algorithm is shown for a test problem in which a laminar flow in a standard shear driven cavity with different Reynolds numbers is considered. The comparison of obtained results for steady state condition with Chen and Ghia's results shows that in addition to high accuracy and convergence, the proposed algorithm leads to more efficient and faster computation than customary BDIMs.

Keywords: radial basis function, vorticity-stream function, BEM, DRM; N-S equations

1. INTRODUCTION

The origins of the boundary element method (BEM) are strongly connected with computation of linear or weakly non-linear field problems, which can be computed by means of boundary-only discretization of computational domain. In case of viscous fluid flows at high values of Reynolds number, the flow phenomena is strongly non-linear and boundary-only discretization had to be paired with domain discretization as well. This procedure weakens the advantages of BEM, in which equations are discretized merely onthe boundary.

In the context of BEM related methods for laminar viscous fluid flows several successful attempts have already been made. An excellent survey of these approaches can be found in the book of Wrobel. These numerical approaches were based on different forms of Navier–Stokes equations, representing the frame for the solution of viscous flow problems. Different techniques of capturing non-linear domain effects were developed, including internal cells, macro-elements and dual and multiple reciprocity methods.

In boundary domain integral method (BDIM), velocity–vorticity formulation was used for the solution of Navier–Stokes equations. Its main advantage is an implicit computation of boundary vorticity values, whereas the disadvantage is the computation of boundary integrals as well as domain integrals.

In obtaining a divergence-free numerical solution for all types of geometry, special attention has to be paid to a proper numerical treatment of governing equations. In case of BDIM, vector potential formulation and vector–velocity formulation of flow kinematics were already used. In the first case in flow kinetics the parabolic-diffusion fundamental solution was used and in the second the diffusion–convection fundamental solution was used.

In order to lower the computational cost of the method, subdomain technique was used with vector–potential formulation, although it was restricted to non-star arrangement of subdomains and to segmentation of flow kinematics. On the other hand, the velocity vector formulation of flow kinematics allowed the use of macro-element based subdomain technique in both flow kinematics and flow kinetics, but it lacked the conservation properties when applied to complex geometries.

In order to overcome these drawbacks, this paper presents a further development of BDIM technique, combining the vorticity-stream function formulation with dual reciprocity method and the use of diffusion–convection fundamental solution. The new computational algorithm can be viewed as a development of the BDIM method which approaches toward the boundary element method over the domain boundary.

2. GOVERNING EQUATIONS

The dimensionless non conservative two-dimensional Navier–Stokes equations in term of the vorticity–stream function formulation within closed domains in Cartesian coordinate system are as follows:

$$\frac{\partial^2\psi}{\partial x^2} + \frac{\partial^2\psi}{\partial y^2} = -\omega \tag{1}$$

$$\frac{\partial \omega}{\partial t} + u\,\frac{\partial \omega}{\partial x} + v\,\frac{\partial \omega}{\partial y} = \frac{1}{\mathrm{Re}}\left[\frac{\partial^2 \omega}{\partial x^2} + \frac{\partial^2 \omega}{\partial y^2}\right] \tag{2}$$

where ω, ψ and Re are the vorticity, stream function and Reynolds number, respectively. u and v are the components of velocity in the x and y directions, which can be calculated using

$$u = \frac{\partial\psi}{\partial y} \quad ; \quad v = -\frac{\partial\psi}{\partial x} \tag{3}$$

One of the advantages of using vorticity-stream function formulation lies in removing pressure gradient terms from the solution process, resulting in a higher numerical stability of the computational scheme. The pressure does not appear in the solution procedure and has no influence on the velocity field, a fact that is of course valid only for incompressible fluid approximation.

3. INTEGRAL EQUATIONS FORMULATION

One of the most important uses of boundary elements method for boundary value problems is the Laplace equation. At first, the formulation and boundary integral equation is presented by weighted residual method. The dual reciprocity method (DRM) is applied to stream function equation. Then the BEM formulation of convection-diffusion equation and descretization procedure is presented. The derivation of the integral form starts with the choice of ϕ^* as the fundamental solution of Laplace equation. Application of the Green's theorem for the equation, the final integral form of Laplace equation is obtained which for the 2-D case becomes

$$C(X')\phi(X') = \int_S \left[\phi^*(X',\mathrm{x})q(\mathrm{x}) - \phi(\mathrm{x})q^*(X',\mathrm{x})\right]dS \quad (4)$$

where C(X')=α/2π and X' is the source point. These parameters are shown in figure 1.

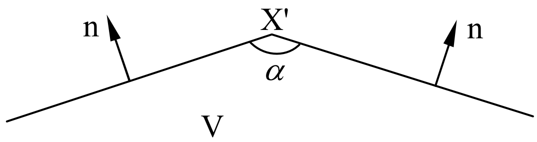

Figure 1 internal angle α at the source point X'

After computation of field variable on the boundary, ϕ and its derivatives are easily obtained in all over the domain:

$$\phi(\mathrm{x}') = \int_S \left[\phi^*(\mathrm{x}',\mathrm{x})q(\mathrm{x}) - \phi(\mathrm{x})q^*(\mathrm{x}',\mathrm{x})\right]dS \quad (5)$$

$$\begin{cases} \dfrac{\partial\phi(\mathrm{x}')}{\partial x} = \int_S \left[\dfrac{\partial\phi^*(\mathrm{x}',\mathrm{x})}{\partial x}q(\mathrm{x}) - \phi(\mathrm{x})\dfrac{\partial q^*(\mathrm{x}',\mathrm{x})}{\partial x}\right]dS \\ \dfrac{\partial\phi(\mathrm{x}')}{\partial y} = \int_S \left[\dfrac{\partial\phi^*(\mathrm{x}',\mathrm{x})}{\partial y}q(\mathrm{x}) - \phi(\mathrm{x})\dfrac{\partial q^*(\mathrm{x}',\mathrm{x})}{\partial y}\right]dS \end{cases} \quad (6)$$

3.1 Numerical implementation

By employing linear elements and dividing the boundary into N_e elements the discretized form of equation (4) is written as

$$C_i\phi_i + \sum_{j=1}^{N_e}\left\langle \begin{bmatrix} h_{i,j}^1 & h_{i,j}^2 \end{bmatrix}\begin{Bmatrix}\phi_j^1 \\ \phi_j^2\end{Bmatrix} - \begin{bmatrix} g_{i,j}^1 & g_{i,j}^2 \end{bmatrix}\begin{Bmatrix}q_j^1 \\ q_j^2\end{Bmatrix}\right\rangle = C_i\phi_i + \sum_{j=1}^{N_e}\left\langle \begin{bmatrix}K_1^j\end{bmatrix}\begin{Bmatrix}\phi_j^1 \\ \phi_j^2\end{Bmatrix} - \begin{bmatrix}K_2^j\end{bmatrix}\begin{Bmatrix}q_j^1 \\ q_j^2\end{Bmatrix}\right\rangle = 0 \quad (7)$$

For computing K_1^j and K_2^j, as shown in Figure (2), the local coordinate ξ-η is employed.

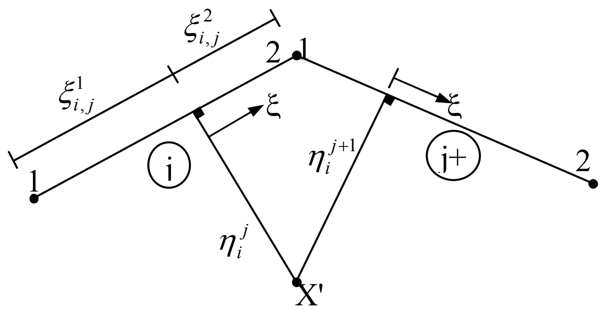

Figure 2 local coordinate for each element

According to the coordinate shown

$$g_{i,j}^k = \int_{S_j}\phi^* N_k dS_j \quad ; \quad h_{i,j}^k = \int_{S_j} q^* N_k dS_j \qquad for \qquad k = 1,2 \quad (8)$$

$$\begin{aligned} K_1^j &= \begin{bmatrix} -I_{11}^j + \xi_{i,j}^2 I_{12}^j & I_{11}^j - \xi_{i,j}^1 I_{12}^j \end{bmatrix} \\ K_2^j &= \begin{bmatrix} -I_{21}^j + \xi_{i,j}^2 I_{22}^j & I_{21}^j - \xi_{i,j}^1 I_{22}^j \end{bmatrix} \end{aligned} \quad (9)$$

where N_1 and N_2 are linear Lagrangian functions and

$$I_{11}^{j}=\frac{1}{l_j}\int_{\xi_{i,j}^1}^{\xi_{i,j}^2}\frac{-1}{2\pi r}\frac{\partial r_{i,j}}{\partial n}\xi d\xi \qquad I_{12}^{j}=\frac{1}{l_j}\int_{\xi_{i,j}^1}^{\xi_{i,j}^2}\frac{-1}{2\pi r}\frac{\partial r_{i,j}}{\partial n}d\xi$$
$$I_{21}^{j}=\frac{1}{l_j}\int_{\xi_{i,j}^1}^{\xi_{i,j}^2}\frac{-1}{2\pi}\ln(r_{i,j})\xi d\xi \qquad I_{22}^{j}=\frac{1}{l_j}\int_{\xi_{i,j}^1}^{\xi_{i,j}^2}\frac{-1}{2\pi}\ln(r_{i,j})d\xi \tag{10}$$

For the employed linear elements, the analytical evaluations of above integrals are presented in the paper of John Wang and Ting-Kuei Tsay (2005).
The integrations should be assembled by

$$G_{i,j}=g_{i,j-1}^{2}+g_{i,j}^{1}$$
$$H_{i,j}=h_{i,j-1}^{2}+h_{i,j}^{1}+C_i\delta_{i,j} \tag{11}$$

By switching the source point over all boundary nodes, N_e equations are obtained. Due to sharp edges at corners, the double node technique is used for flux discontinuity. Hence the G and flux vector are matrices of rank $N_e\times(N_e+4)$ and (N_e+4) respectively.
In equation (1) ω is treated as body force. The integral form of equation (1) is written as

$$C(X')\phi(X')=\int_S\left[\phi^*(X',\mathrm{x})q(\mathrm{x})-\phi(\mathrm{x})q^*(X',\mathrm{x})\right]dS$$
$$+\int_V\phi^*(X',\mathrm{x})\omega(\mathrm{x})\mathrm{dV} \tag{12}$$

which has one extra domain integral term over equation (4) and can be computed by dividing the domain to some virtual cells and computed numerically. These cells are called background cells. This type of domain calculation removes the BEM advantage that all equations and computations are done on boundary. Therefore to approximate these terms the DRM (dual reciprocity method) is employed.

4. DRM (DUAL RECIPROCITY METHOD)

This method was first introduced by Nardini & Brebbia and then developed for some applications. In fact this method is the generalization of particular solutions method. By the DRM, ψ is written as $\psi=\tilde{\psi}+\hat{\psi}$, in which $\tilde{\psi}$ is the $\nabla^2\tilde{\psi}=0$ solution and $\hat{\psi}$ is the particular solution of $\nabla^2\hat{\psi}=-\Omega$ which is approximated by a $\hat{\psi}_k$ series. The series has N+L terms in which N is the number of boundary nodes and L is number of some internal nodes. According to the approximation, we have

$$\omega\cong-\sum_{k=1}^{N+L}\alpha_k f_k \tag{13}$$

α_k are coefficients that are unknown at first and f_k are approximation functions. $\hat{\psi}_k$ and f_k are related by

$$\nabla^2\hat{\psi}=f_k \tag{14}$$

Substituting equation (14) and (13) in equation (1), one obtains

$$-\sum_{j=1}^{N_e}\int_{S_j}\left[\psi^*(X',\mathrm{x})q(\mathrm{x})-\psi(\mathrm{x})q^*(X',\mathrm{x})\right]dS+C(X')\psi(X')$$
$$=\sum_{k=1}^{N+L}\alpha_k\left[C(X')\hat{\psi}_k(X')-\sum_{j=1}^{N_e}\int_{S_j}\left[\psi^*(X',\mathrm{x})\hat{q}_k(\mathrm{x})-\hat{\psi}_k(\mathrm{x})q^*(X',\mathrm{x})\right]dS\right] \tag{15}$$

After integrating, the equation can be rewritten as

$$\sum_{j=1}^{N}H_{i,j}\psi_j-\sum_{j=1}^{N}G_{i,j}q_j=\sum_{k=1}^{N+L}\alpha_k\left(\sum_{j=1}^{N}H_{i,j}\hat{\psi}_{j,k}-\sum_{j=1}^{N}G_{i,j}\hat{q}_{j,k}\right) \tag{16}$$

G and H are the matrices defined in equation (11). Applying the above equation for all boundary nodes we obtain

$$H\Psi - GQ = (H\hat{U} - G\hat{Q})\alpha \tag{17}$$

Equation (17) is the base equation in our DRM implementation. As can be seen in the equation, by considering L=0 the equations are fully evaluated over boundary. The more the interior nodes are considered, the higher the accuracy would be. By evaluating the vorticity in N+L nodes, vector α is obtained by $\omega = \mathrm{F}\alpha$

Substituting the above equation of α in equation (17) yields

$$H\Psi - GQ = (H\hat{U} - G\hat{Q})\mathrm{F}^{-1}\omega \tag{18}$$

Selecting approximation functions fj is still an open subject. The accuracy of polynomial functions is higher. In using polynomial functions, F may be singular and consequently not invertible. Radial basis functions are proved to avoid singular F matrix. Hence Radial basis functions (RBF) are employed in this study. For more details on RBFs the reader can refer to works of Kansa, powell and wendland. The parameters in RBFs are called shape parameters and are used for fine tuning. In this research the Hardy Multiquadric is employed with c=1.

5. VORTICITY TRANSFER EQUATION

To solve equation (2) the homogenous form of the equation is coupled with DRM. Consequently the formulation of homogenous equation is presented and then temporal term is descretized by another technique. Solution of convection-diffusion equations by BEM shows promising results. Applying divergence theorem to steady state form of equation (2) one obtains

$$\int_V \omega(\nabla^2\omega^* + u\,\mathrm{Re}\frac{\partial\omega^*}{\partial x} + v\,\mathrm{Re}\frac{\partial\omega^*}{\partial y}dV = \int_S(\omega\frac{\partial\omega^*}{\partial n} - \omega^*\frac{\partial\omega}{\partial n})dS + \mathrm{Re}\int_S \omega\omega^*\mathrm{V}_n dS \tag{19}$$

By considering ω^* as the fundamental solution, the final form of equation (19) is written as

$$\omega(\mathrm{X}') = \frac{1}{\mathrm{Re}}\int_S \omega^*(\mathrm{X}',\mathrm{x})\frac{\partial\omega}{\partial n}dS - \frac{1}{\mathrm{Re}}\int_S \omega(\mathrm{x})\frac{\partial\omega^*(\mathrm{X}',\mathrm{x})}{\partial n}dS - \int_S \omega^*(\mathrm{X}',\mathrm{x})\omega(\mathrm{x})V_n(\mathrm{x})dS \tag{20}$$

where K_0 and K_1 are second order Bessel functions and

$$\omega^* = \frac{\mathrm{Re}}{2\pi}K_0(\mu r)\exp\left(\mathrm{Re}\frac{\vec{\mathrm{V}}.\vec{\mathrm{r}}}{2}\right) \text{ where } \mu = \mathrm{Re}\frac{|\mathrm{V}|}{2} \tag{21}$$

Source point is considered on all boundary nodes. Hence

$$C(\mathrm{X}')\omega(\mathrm{X}') = \frac{1}{\mathrm{Re}}\int_S \omega^*(\mathrm{X}',\mathrm{x})\frac{\partial\omega}{\partial n}dS - \int_S \omega(\mathrm{x})F^* dS \tag{22}$$

in which F^* is the total flux defined as

$$F^* = \frac{1}{\mathrm{Re}}\frac{\partial\omega^*}{\partial n} + \mathrm{V}_n\omega^* = \frac{1}{2\pi}\left[-\mu K_1(\mu r)\frac{\partial r}{\partial n} + \mathrm{Re}\frac{\mathrm{V}_n}{2}K_0(\mu r)\right]\exp\left(\mathrm{Re}\frac{\vec{\mathrm{V}}.\vec{\mathrm{r}}}{2}\right) \tag{23}$$

The implementation and descretization is done as before. The temporal descretization is done by a method based on Adams method. Integration of equation (2) in time results in

$$\omega^{n+1} - \omega^n = \int_{t^n}^{t^{n+1}} \frac{1}{\mathrm{Re}}\nabla^2\omega\,dt - \int_{t^n}^{t^{n+1}} (\vec{\mathrm{V}}.\vec{\nabla})\omega\,dt \tag{24}$$

The integral with linear term is evaluated by implicit Adams-Moulton while the one with non linear term is evaluated by explicit Adams-Bashford. Consequently the equation of r^{th} order is

$$\omega^{n+1} - \omega^n = \Delta t\sum_{j=0}^{r-1}\frac{1}{\mathrm{Re}}\beta_j^1\left(\nabla^2\omega\right)^{n+1-j} - \Delta t\sum_{j=1}^{r}\beta_j^2\left(\vec{\mathrm{V}}^{n+1-j}.\vec{\nabla}\right)\omega^{n+1-j} \tag{25}$$

In this study the Adams 2 is employed. Hence the equation is rewritten as

$$\frac{1}{\text{Re}}\nabla^2\omega^{n+1} - (\vec{\text{V}}^{\,n+1}.\vec{\nabla})\omega^{n+1} = f(\vec{\text{V}}^{\,n},\omega^n,\omega^{n+1}) \tag{26}$$

The above formulation is coupled with DRM and solved in each time step. The method is an iterative method and in each time step iteration goes on until the below criterion is satisfied

$$\left|\frac{\omega^{n+1}{}_{k+1} - \omega^{n+1}{}_{k}}{\omega^{n+1}{}_{k+1}}\right| < \varepsilon_{\text{relative}} \tag{27}$$

$\varepsilon=10^{-6}$ is considered. By solving the equation (26) in time step (n), the vorticity values are obtained. Hence equation (17) can readily be solved. By solving equation (17) the ψ values are computed on the boundary and some limited nodes in the domain. By having stream function, the vorticity boundary conditions and velocity components can be computed. These boundary conditions are used to solve vorticity equation in the next iteration, i.e. in a sequential manner. This process continues until the convergence criterion (27) is satisfied.

6. BOUNDARY CONDITIONS

Driven cavity flow problem is one of the best benchmarks to verify numerical models. According to Ghia and Shin, the vorticity boundary condition does not exist explicitly and should be constructed. The method is based on Taylor series second order expansion. By some mathematical operations on Taylor series with consideration to equation (3), the following second order boundary conditions are obtained

$$\omega_{1,j} = \frac{\psi_{3,j} - 8\psi_{2,j} + 7\psi_{1,j}}{2(\Delta x)^2} \quad \text{(Left)} \qquad \omega_{IM,j} = \frac{\psi_{IM-2,j} - 8\psi_{IM-1,j} + 7\psi_{IM,j}}{2(\Delta x)^2} \quad \text{(Right)}$$
$$\omega_{i,1} = \frac{\psi_{i,3} - 8\psi_{i,2} + 7\psi_{i,1}}{2(\Delta y)^2} \quad \text{(Bottom)} \qquad \omega_{i,JM} = \frac{\psi_{i,JM-2} - 8\psi_{i,JM-1} + 7\psi_{i,JM}}{2(\Delta y)^2} - \frac{3}{\Delta y}U \quad \text{(Top)} \tag{28}$$

As can be seen, two other layers of nodes parallel to boundary nodes are entered in above equation. It should be noted that these nodes are also included in DRM method. Three different meshes used in implementation are illustrated in figure 4. For stability purposes, $\Delta t=10^{-3}$ is considered. At the initial time the fluid is at rest.

7. SOLUTION METHOD AND ALGORITHM

In each time step, equations (1) and (2) are solved in an iterative manner and again this procedure is done until criterion (27) is achieved for all boundary nodes. Two loops are employed. The outer loop is for time steps while the inner one is for iteration in each time step. For stability purposes, the SUR (successive under relaxation) parameter is employed. To assess error, the criterion below is used

$$\Pi = \frac{\sum_{j=1}^{N_e}\left({}^{k+1}\{\omega_j\} - {}^{k}\{\omega_j\}\right)^2}{\sum_{j=1}^{N_e}\left({}^{k+1}\{\omega_j\}\right)^2} \tag{29}$$

According to figure (4), the relaxation parameter for t=6 sec and mesh = 45×45 with $\Pi=10^{-5}$ was determined to be about 0.63 which led to 28 iteration. It is worth mentioning that the iteration numbers decrease as time of modeling increases. For t=6 sec and mesh = 45×45 with relaxation factor of 0.63,t he convergence of the proposed method is plotted in figure (3).

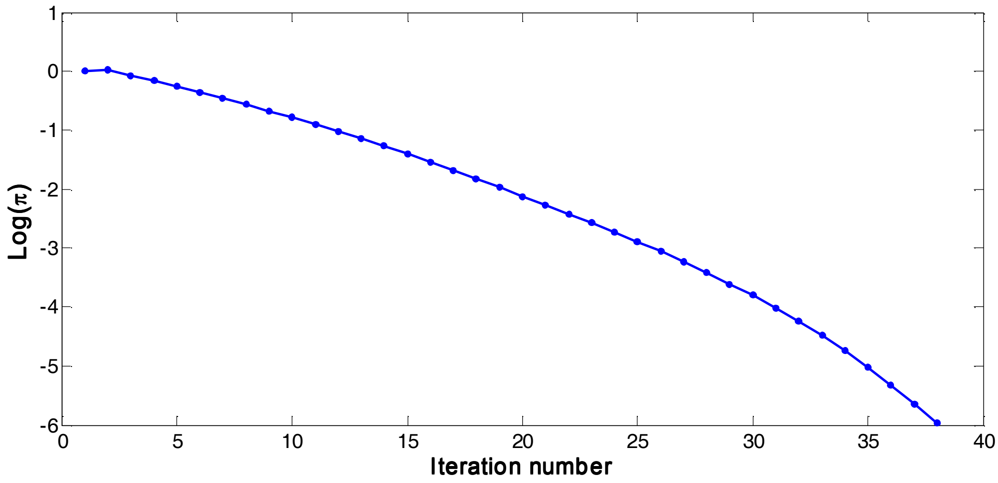

Figure 3 The convergence in t=6 for Re=1000

8. THE RESULTS AND CONCLUSION

In higher Reynolds number the swirling nature of flow intensifies. To model higher values of Reynolds number, three node distributions are considered which are 27×27, 45×45 and 61×61. These node distributions, which are displayed in figure 4, are utilized to model Reynolds numbers up to Re=100, 1000 and 2000, respectively.

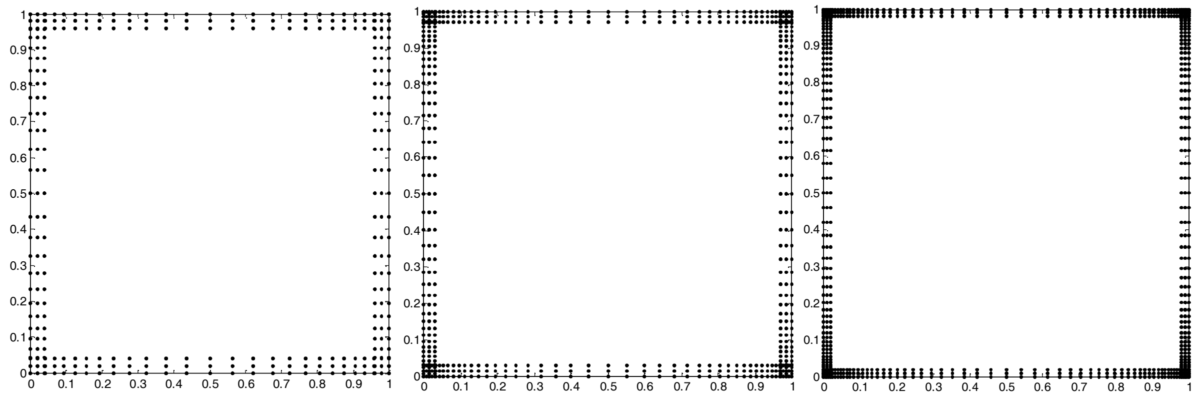

Figure 4 Cavity with three different meshes

The primary vortex and vortex produced in two corners are listed in table (1). Also computation CPU time relative to BDIM is presented in the last column which shows the advantage, i.e. faster and less computationally expensive algorithm than regular BDIM.

Table 1 Coordinates of vortices in steady state

Mesh	Re	Primary vortex	Right bottom	Left bottom	Relative CPU time
27×27	400	0.61,0.7 5	---	---	0.28
45×45	100	0.62,0.73	---	---	
	400	0.57,0.68	0.88, 0.10	---	0.052
	1000	0.54,0.7 2	0.86, 0.11	0.07,0.06	
61×61	2000	0.52,0.5 5	0.87, 0.98	0.08,0.09	0.029

To display the transient solution of flow, the time history of streamlines for Re=2000 is demonstrated in figure (5). At the starting times the vortex is near the upper wall and enlarges smoothly moving toward the upper left corner. As shown in about t=6 seconds the first secondary vortex is produced at right of the cavity at about y=0.5. The secondary vortex then enlarges and moves toward the bottom right corner of cavity, whereas the primary vortex moves from the upper right corner to the centre of the cavity. According to figures, at higher time values, the streamlines change slower than that of starting times. The streamlines seem to reach the steady-state at about t=90 seconds.

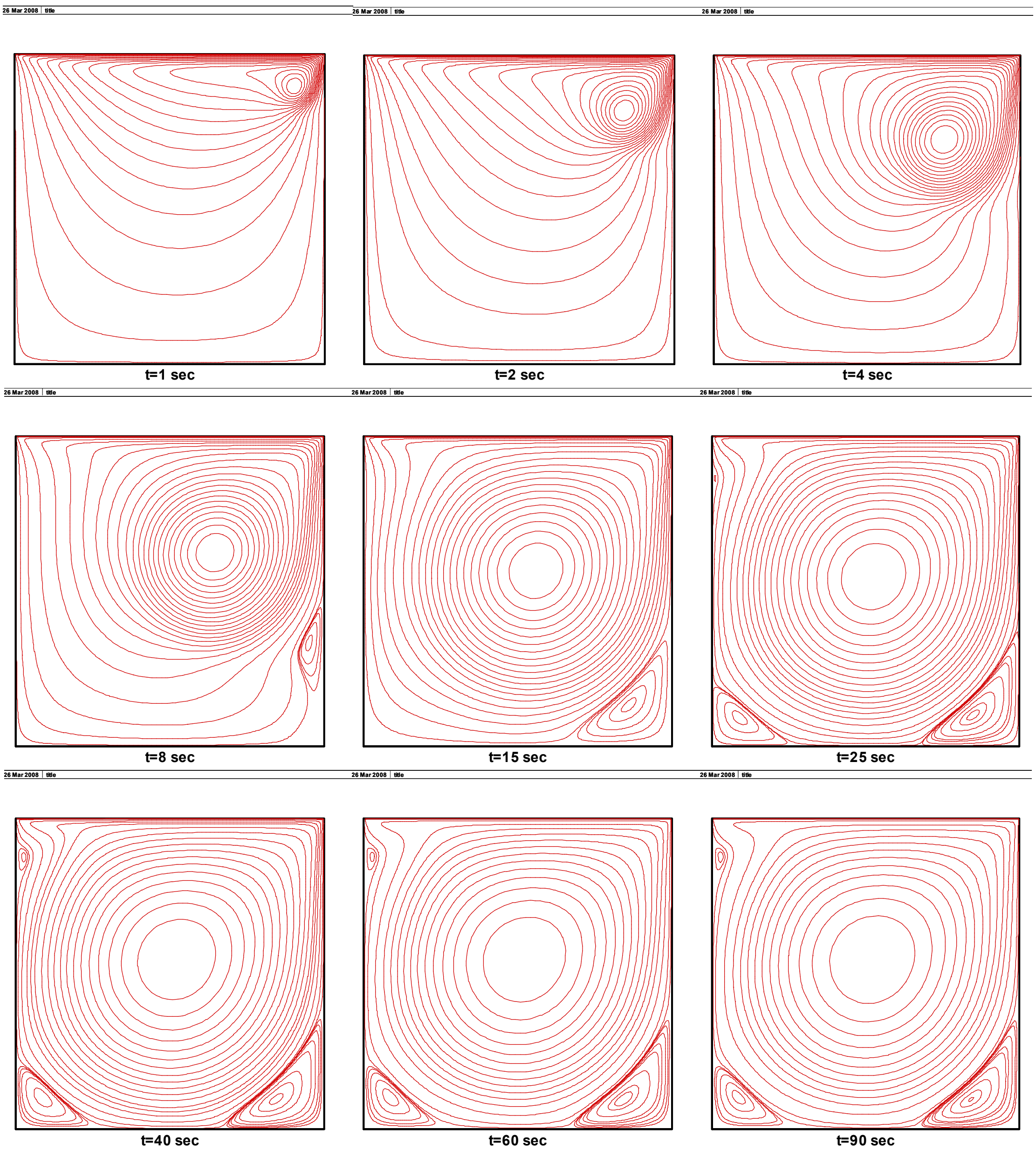

Figure 5 Time history of streamlines for Re=2000 in boundary mesh of 61×61

The above figures clearly show the flow nature, i.e. the swirling behaviour of flow in high Reynolds numbers. To verify the solutions, results from current modified BEM are compared to that of Ghia & Shin. In that article they presented the steady state solution of velocity components on horizontal and vertical centrelines and vorticity on the top wall for different Reynolds number. Hence, steady state velocity field distributions at x=1/2 (in y direction) and at y=1/2 (in x direction) are plotted in figures (6a) and (6b), respectively, and are compared with Ghia (1992) and chen's (1991) results. Also, in order to observe the convergence speed of flow to steady-state, the vertical velocity distributions on the horizontal centreline (y=0.5) are plotted in figure 7.

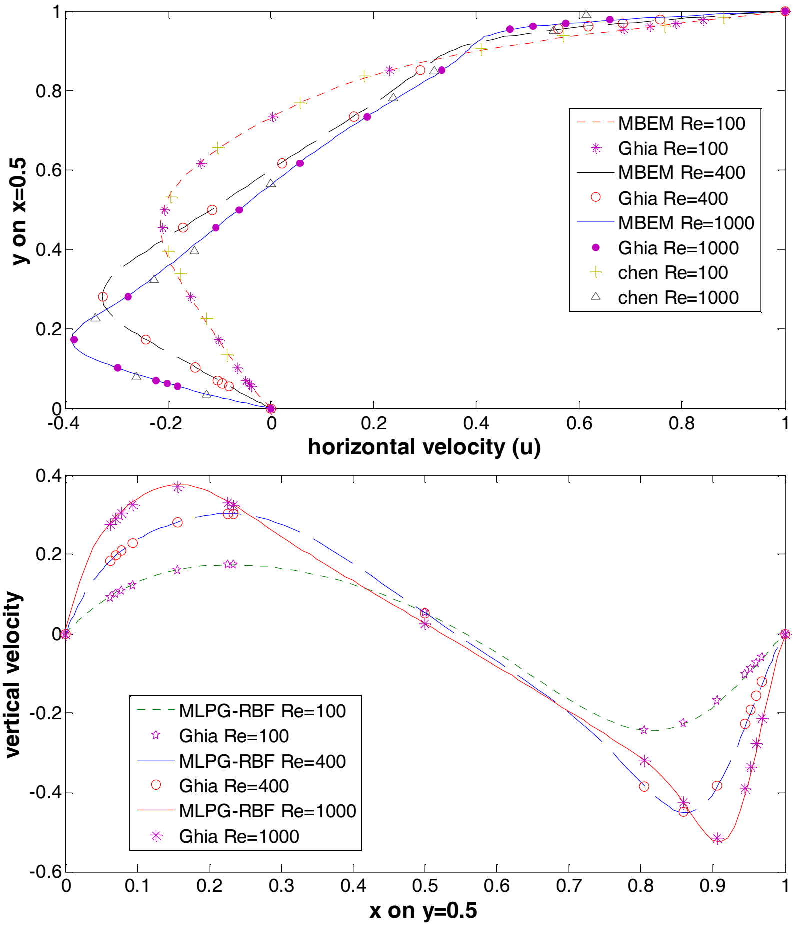

Figure 6 Comparison of vertical and horizontal component of velocity in x=1/2 and y=1/2 with Ghia & Chen results

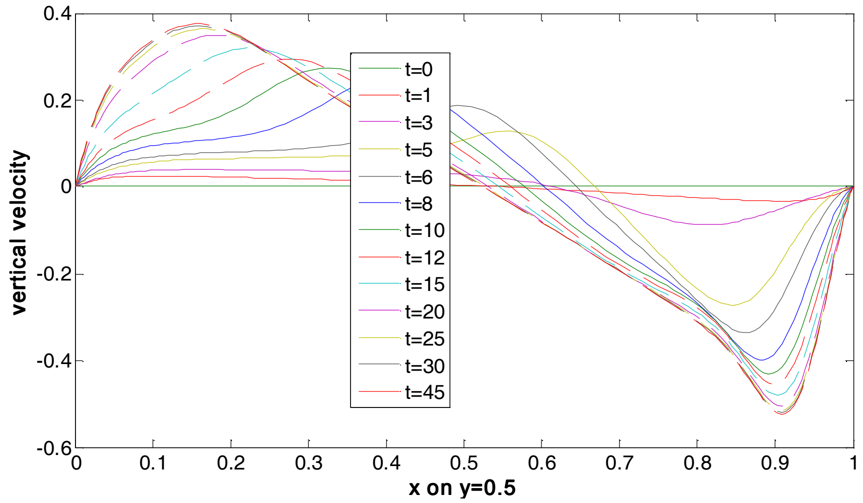

Figure 7 Transient vertical velocity on y=1/2 for Re=1000

Comparison of the results for different Reynolds numbers, shown in figure 6, shows promising results and proves the excellent method capability. Figure 7 clearly shows that at starting times velocity changes rapidly whereas the change rate becomes gradually less and eventually reaches to a fixed curve, which corresponds to the steady state condition. The figure also shows that the flow reaches to steady state at about t=45 seconds.

9. CONCLUSION

As shown in this paper the new proposed method for two-dimensional analysis for transient fluid flows is well verified by certified results. The robustness was verified by considering the well-known CFD problem, lid driven cavity flow, which was shown to let to promising results. The method is capable of reducing computation expenses since equations are satisfied on some boundary nodes and some finite layers of nodes adjacent to boundary nodes. Hence, it is an efficient method for especially transient problems and a powerful alternative to BDIM.

REFERENCES

Florez, W.F. and Power H. (2001), Comparison between continuous and discontinuous boundary elements in the multidomain dual reciprocity method for the solution of the two-dimensional Navier–Stokes equations, *Engrg. Anal. Bound. Elem*., 25, 57–69

Ingber, M.S. (2003), A vorticity method for the solution of natural convection flows in enclosures, *Int. J. Numer. Methods Heat Fluid Flow*, 13, 655–671

Skerget, L. S. and Hribersek, M. and Kuhn, G. (1999), Computational fluid dynamics by boundary domain integral method, *Int. J. Numer. Methods Engrg*. 46 (1999) 1291–1311.

powell, M.J.D. (1992), The theory of radial basis function approximation, Vol. II, *Oxford Science Publications*

Wrobel, L.C. (2002), Applications in thermo-fluids and acoustics. *The Boundary Element Method, vol. 1, Wiley*, New York

Grigoriev, M.M. and Dargush, G.F. (1999), A poly-region boundary element method for incompressible viscous fluid flows, *Int. J. Numer. Methods Engrg*. 46, 1127–1158.

Nardini, N. and Brebbia, C.A. (1982), A new approach to free vibration analysis using boundary elements, Boundary Element Methods in Engineering, *Computational Mechanics Publications, Southampton, and Springer-Verlag, Berlin*

Patridge, P.W. and Brebbia, C.A.. and Wrobel, L.C. (1992), The dual Reciprocity Boundary Element Method, *Computational Mechanics Publications*, Southampton

John Wang, Ting-Kuei Tsay (2005), Analytical evaluation and application of the singularities in boundary element method, *Engineering Analysis with Boundary Elements*, 29,241– 256

Ghia, U. and Ghia, K.N. and Shin (1982), 'High-Re solution For Incompressible Flow Using The Navier-Stokes Equation And Multigrid Method, *Journal Of Computational Physics*, 48, 387-411

Wendland, H. (1999), On the smoothness of positive definite and radial functions, *Journal Comput. Appl. Math*., 101, 177-188

Wrobel, L.C. and DeFigueiredo, D.B. (1991), Numerical analysis of convection-diffusion problems using the boundary element method, *International Journal of Numerical Methods for Heat & Fluid Flow*, 1, 3-18

Franke C., Schaback R. (1998), Solving partial differential equations by collocation using radial basis functions, Appl. Math. Comput., 93, 73-82.